Tribology International 44 (2011) 1819–1826

Contents lists available at ScienceDirect

Tribology International

journal homepage: www.elsevier.com/locate/triboint

Friction of molybdenum disulfide–titanium films under cryogenic vacuum conditions

C.G. Dunckle *, M. Aggleton, J. Glassman, P. Taborek

Department of Physics and Astronomy, University of California, Irvine, Irvine, CA 92697, USA

ARTICLE INFO

Article history:
Received 6 June 2011
Received in revised form
18 July 2011
Accepted 21 July 2011
Available online 7 August 2011

Keywords:
Friction
Low temperature
Ultra-high vacuum
Molybdenum disulfide

ABSTRACT

The tribological behavior of steel and sapphire sliding on a sputtered MoS_2+Ti coating was studied in ultra-high vacuum as a function of temperature over the range of 4–300 K. The coefficient of kinetic friction for the steel/moly interface was determined to be approximately 0.05 from room temperature to 240 K, and increased monotonically to 0.125 at 4 K. The sapphire/moly friction coefficient was measured to be 0.15 ± 0.05 at room temperature and increased monotonically to 0.25 at 4 K. We also analyze in detail the flash temperature due to frictional heating at the sliding contacts. Flash heating is a particularly strong effect at cryogenic temperatures.

1. Introduction

In many engineering applications ranging from aerospace to MEMS devices, conventional fluid lubricants cannot be used. Sliding contacts in these situations are typically lubricated with dry, solid lubricants such as graphite, PTFE [1], or molybdenum disulfide [2]. In vacuum applications at room temperature and above, MoS_2, particularly when combined with various metal fillers, is known to provide low coefficients of friction as well as low wear rates [3]. Devices which combine mechanical motion and low temperatures often work in vacuum to avoid condensation and the build-up of frost. Despite this device-driven requirement, there is very little data on the performance of MoS_2 in cryogenic vacuum environments [4,5]. Most previous cryogenic measurements have used sliding surfaces in direct contact with a liquid or gaseous cryogens [6–9]. Friction in these systems involves the hydrodynamics of lubrication and possibly boiling, and is quite different from dry sliding friction in vacuum. The only vacuum cryogenic measurements we are aware of for MoS_2-based composites [5,10] provide data for only a few isolated temperatures and find almost no change in frictional behavior between room temperature and cryogenic temperatures. These results must be interpreted cautiously because of the potentially strong effects of localized frictional heating at the contact points.

In addition to the practical engineering issues, characterizing the low temperature behavior of the friction coefficient also provides valuable insight into the fundamental mechanisms of friction. Although a comprehensive theory of the temperature dependence of friction does not exist, the temperature dependence of several specific mechanisms has been explored. Phonon mediated processes are expected to freeze out at low temperature, which could lead to a low friction state at low temperature [11]. Thermally activated processes such as bond breaking associated with sliding have been investigated in single-contact models and are theoretically expected to lead to high friction states at low temperatures [12]. Single contact measurements made with Atomic Force Microscopy (AFM) show various material/geometetric dependent behavior that, in some cases, result in abrupt increases in friction at temperatures near 100 K [13–15] while other measurements show a more gradual temperature dependence [16,17]. The use of Quartz-crystal microbalances have also contributed to low temperature investigations of friction [18,19]. Molecular dynamics simulations typically show a friction coefficient which increases gradually as the temperature is decreased to cryogenic levels [17,20,21].

In this paper we report measurements using a sliding block tribometer in a cryogenic vacuum environment that show the friction coefficient of MoS_2+Ti coatings increases as the temperature is lowered from room temperature. The counterfaces were spherical bearings made of either stainless steel or sapphire. These materials are both of engineering interest, and have dramatically different thermal, mechanical, and electrical properties. The results are reported as a function of the temperature of the substrate, but the temperature of the contact can be substantially higher. Below we analyze the temperature rise at the contact point due to fictional heating. Measurements of temperature dependent friction on other materials using the same

* Corresponding author.
E-mail address: cdunckle@uci.edu (C.G. Dunckle).

0301-679X/$ - see front matter © 2011 Elsevier Ltd. All rights reserved.
doi:10.1016/j.triboint.2011.07.010

apparatus are reported in Burton et al. [22] and Aggleton et al. [23].

2. Experiment

The coating tested for this experiment was a 1 μm thick film of molybdenum disulfide + titanium on a stainless steel substrate with a peak to peak roughness of approximately 80 nm over a length of 30 μm. The coating was produced by Teer Coatings Ltd. using DC magnetron sputtering with an initial titanium interlayer and subsequent simultaneous sputtering from three MoS_2 targets and one titanium target. Titanium is added to strengthen the normally soft MoS_2 coating, increasing the wear lifetime. As observed by Barton and Pepper [24], molybdenum disulfide produces transfer films on stainless steel in sliding distances on the centimeter length scale. Similar transfer film formation is expected in coatings with added titanium and experimental results [25] are in agreement with this supposition. Further details on coating fabrication are described elsewhere [25,26].

The sliding block tribometer used in this experiment is mounted in a vacuum can containing two nickel-plated copper radiation shields equipped with aligned optical windows. The aligned windows allow for visible operation of the tribometer. The shields are bolted to copper plates that are separately fixed to the two cooling elements of a closed cycle, pulsed tube refrigerator. The shields cool to minimum temperatures of <40 K and <4 K respectively and allow the tribometer to reach a minimum temperature of 4 K. An average vibrational displacement of ~ 1 μm was measured using an accelerometer situated atop the vacuum can in close proximity to the active refrigerator head.

The track of the tribometer is supported by mechanical arms fixed to the refrigerator's terminal cooling element. Conductive heat transfer by physical connection to the 4 K copper plate cools the tribometer. The tribometer slider consists of a copper block (0.8 in × 0.5 in × 0.5 in) and six stainless steel or sapphire bearings (1/8 in dia.) attached to two adjacent sides of the block. The bearings serve as counter faces to a vee-track of stainless steel plates coated with the previously described MoS_2 + Ti coating (Fig. 1). A solenoid attached to one end of the track is used to magnetically pin the slider to that end by means of a small mu-metal button threaded into the copper block. Mu-metal was chosen because it has no remaining magnetization after exiting a magnetic field. This property removes the possible influence of eddy currents during the descent of the block. The supporting structure of the track is equipped with a heater and a silicon diode thermometer (LakeShore) to monitor and control the temperature of the tribometer. A mechanical feedthrough allows for the rotation of the tribometer into position such that the slider can be pinned to the solenoid and set to a fixed angle for sliding. Spring loaded bumpers are built into the ends of the track to reduce the vertical bouncing caused by impact at the end of each slide and during rotation. A more detailed description of the apparatus can be found in Burton et al. [22].

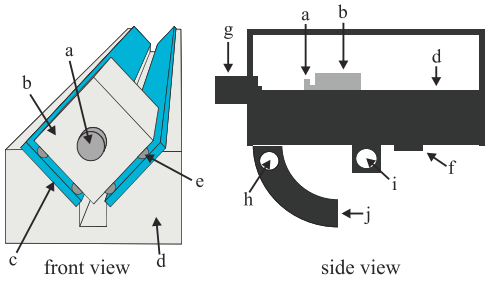

Fig. 1. Schematic of the sliding tribometer: a, mu-metal button; b, copper slider; c, molybdenum disulfide + titanium coated tracks; d, copper vee-track base; e, stainless steel or sapphire bearing counterfaces; f, thermometer; g, solenoid; h, heater; i, pivot; j, counterweight.

A wear-in procedure was performed in air until a repeatable room temperature measurement was obtained. The resulting value of $\mu = 0.06$ for the steel/moly interface shown in Fig. 2 is in good agreement with the measurements made by Teer [25]. A similar wear-in process was done for the sapphire/moly interface, but the results showed much larger fluctuations in the values with μ in the range of 0.1–0.25 (Fig. 3). The stochastic behavior appears to be a result of transfer film dynamics of the molybdenum disulphide with the sapphire. Though this behavior is also apparent in the temperature dependent measurements, clear trends are observed and confirmed by repeated measurements taken during temperature cycling.

High speed video (1000 frames per second using a Phantom 7.2 camera) is triggered to record the slide of the block when the solenoid is switched off. The motion of the block is monitored by using edge tracking software that measured the position of the block as a function of time. The acceleration of the block is determined by fitting a parabola to the block's trajectory. The normal force on each of the two faces in contact with the track is given by

$$F_N = \frac{\sqrt{2}}{2} mg \cos\theta \tag{1}$$

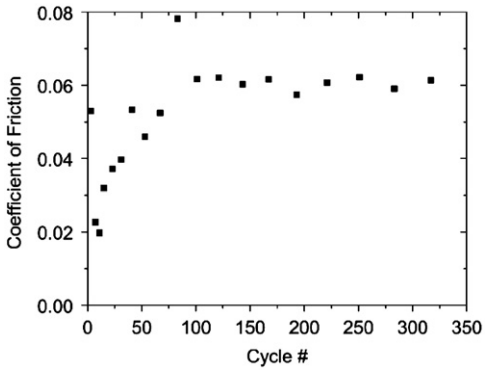

Fig. 2. Wear-in process for steel on MoS_2 + Ti interface at room temperature and pressure. Steady state friction is observed to be at $\mu = 0.06$. This is in agreement with previously published results [25,31].

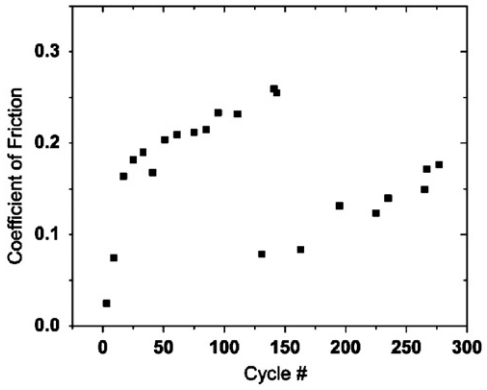

Fig. 3. Wear-in process for sapphire on MoS_2 + Ti interface at room temperature, pressure and humidity. The coefficient of friction initially rises to 0.25 where a transition occurs returning it to a low friction state of 0.1 from which it slowly returns to a high friction state. This behavior is presumably related to transfer film dynamics resulting from the sapphire contact material and relatively low contact pressures in this experiment. The higher coefficient relative to the steel interface is in agreement with previous results [27].

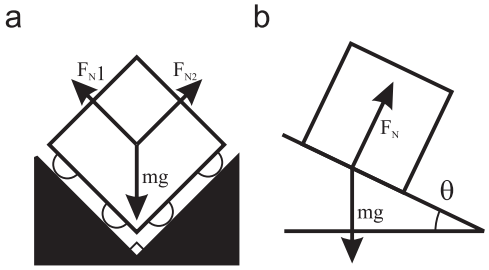

Fig. 4. The normal force on the block from the track has contributions from (a) the vee-track shape and (b) the angle the track is tilted for the block to slide. This contributes factors of $\sqrt{2}/2$ per interface and $\cos\theta$ giving a total normal force of $F_N = \sqrt{2}mg\cos\theta$.

where m is the mass of the block, g in the acceleration due to gravity and θ is the angle that the track is tilted from the horizontal (Fig. 4). The factor of $\sqrt{2}/2$ arises from the vee shape of the track. Assuming five points of contact based upon the necessary spacial constraints on the sliding block,[1] the total normal force is 0.375N, or 0.075N per point of contact. Using this normal force and the acceleration of the block down the track, the coefficient of kinetic friction, μ, of this system is given by

$$\mu = \frac{1}{\sqrt{2}\cos\theta}\left(\sin\theta - \frac{a}{g}\right) \tag{2}$$

where a is the measured acceleration, g is acceleration due to gravity, and θ is the angle of the track with respect to the horizontal. The angle is in general adjustable, but is fixed for this experiment at approximately 25° and determined exactly during image processing. The Hertzian contact area based on five points of steel on steel contact using the physical dimensions of the system as well as the Young's modulus of steel is calculated to be 265 μm^2 per contact. Each sliding event lasts for approximately 0.2 s with the calculated coefficient of kinetic friction in Eq. (2) representing the mean value over each slide event. After each event, the solenoid is re-activated and the track is rotated to reset the block to its starting position and angle.

During the initial cooling process the tribometer was thermally regulated above 300 K while the walls of the cryostat cooled to their minimum operating temperatures. The system was maintained in this state for several hours before any further measurements were taken to remove adsorbates from the sliding surfaces. The pressure in this system cannot be measured directly since ion gauges and surface spectroscopy methods generate a large heat load onto the inner shield increasing the lowest achievable temperature. Nevertheless, the effective pressure in our apparatus is far below the values of 10^{-10} Torr typical of room temperature UHV systems because the tribometer is completely surrounded by surfaces at a few Kelvin serving as a strong cryopump that permanently traps all species except helium. Similar systems in our lab have been used to keep extremely reactive surfaces such as cesium and rubidium atomically clean for months [28,29]. The weak thermal connection of the track to the cryostat through the supporting mechanical arms allows for maintaining its temperature above 300 K by dissipating <1 W into the attached heater without drastically affecting the shield temperature. Any material adsorbed onto the surfaces of the tribometer can be pumped away at a rate determined by the binding energy of the adsorbate and the temperature of the sliding surface. A kinetics calculation for a surface at 300 K shows that species with a binding energy below approximately 100 kJ/mole will be pumped away, while species with a higher binding energy will remain on the surface during the time scale of our experiment. Water is of particular concern in this experiment as it can have a significant effect on the tribological behavior of MoS_2. A change in the relative humidity from 0 to 50% induces up to a factor of 5 increase in the coefficient of friction [30,31]. The binding energy of water spans the range of 25–60 kJ/mole depending on the surface. Temperature programmed desorption studies [32–34] show that water and ice rapidly desorb between 130 K and 180 K. Holding the temperature of our tribometer above 300 K for several hours while preparing the cryogenic UHV environment ensures that the coverage of water on the tribological surfaces is negligible.

After run-in and adsorbate removal the heat applied at the base of the tribometer was reduced, allowing the temperature to slowly decrease over the course of approximately a day. Data were gathered as the temperature decreased from 300 K to 4 K with the temperature measured at the bottom base of the track (Fig. 1). Measurements were repeated as the temperature of the tribometer was cycled between room temperature and 4 K while maintaining the temperature of the surrounding radiation shield at 4 K.

Friction generates a heat flux resulting in a local increase in the temperature near the contact points known as "flash heating". For this reason, a macroscopic thermometer several centimeters from the contact point will not provide an accurate measurement of the temperature at the microscopic contact. The general principles to estimate the difference between the measured macroscopic temperature and the local temperature at the contact point induced by dissipative heating have been studied in some detail [35–39]. If the contact point is moving so slowly that it can be regarded as stationary, the problem reduces to calculating the temperature in a half space with a uniform heat flux q inside a disk of radius R and zero outside the disk with the additional boundary condition that the temperature is zero far from the disk; the analytic solution to this problem is

$$T(r,z) = \frac{qR}{\kappa}\int_0^\infty e^{-\lambda z}J_0(\lambda r)J_1(\lambda R)\frac{d\lambda}{\lambda} \tag{3}$$

The maximum temperature at the center of the disk from this result is

$$T_{max} = \frac{Rq}{\kappa} \tag{4}$$

The temperature field for the stationary case, shown in Fig. 5, is symmetric about the z-axis and relaxes to the background value for distances greater than 2 or 3 times R. For the case more applicable to this experiment that of a contact point moving with velocity U, the leading edge of the disk will be in contact with colder regions of the substrate, and the trailing edge will be in contact with previously heated regions. This differential thermal landscape induces an asymmetric temperature profile. The degree of asymmetry is governed by the relative rates at which heat diffuses from the contact and is advected by the moving contact. The time required for heat to diffuse a distance R is R^2/χ, where χ is the thermal diffusivity with SI units of m^2/s. The time required for the source to move a distance equal to the diameter of the disk is $2R/U$, and the ratio of the two times is a dimensionless number $Pe = RU/2\chi$ called the Peclet number. If $Pe > 1$, the motion of the contact produces noticeable asymmetry of the temperature distribution; the numerical results for this case are presented in [40]. In our experiment, the size of the Hertzian contact is $R = 9$ μm, and the maximum velocity is $U = 0.72$ m/s. The thermal properties of

[1] A rigid body in three dimensions has six degrees of freedom: three translational and three rotational. Five of the block's degrees of freedom are constrained in this experiment requiring a minimum of five points of contact from five independent bearings. An additional contact point is either redundant or overconstrains the system preventing sliding. For the analysis in this paper we assume the sixth bearing is not in contact.

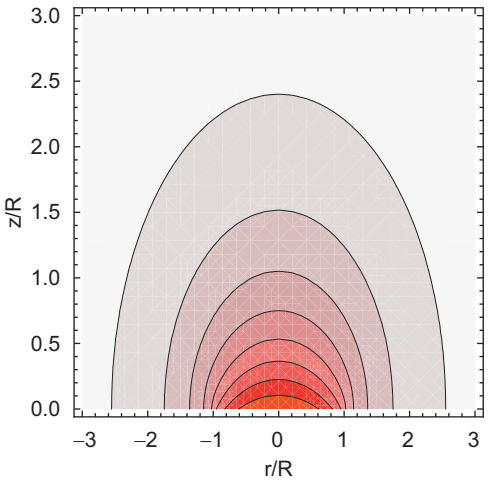

Fig. 5. Contour plot of the temperature for a constant stationary heat flux on a disk of radius R in the r–z plane through the center of the disk. The contour lines are at intervals of 0.1 of the maximum temperature given by Eq. (4).

Table 1
Temperature dependence of thermal diffusivity and Peclet number [41,42].

Temperature (K)	Thermal diffusivity (m^2/s)		Max. Peclet number	
	Sapphire (10^{-4})	Steel (10^{-6})	Sapphire	Steel
4	25 000	17.2	1×10^{-10}	0.18
50	675	10.1	5×10^{-9}	0.32
100	7.8	5.0	4×10^{-7}	0.64
200	0.44	4.8	7×10^{-6}	0.68
300	0.11	4.2	3×10^{-5}	0.78

the materials vary with temperature, as shown in Table 1, but the Peclet number for both steel and sapphire is always less than 0.78, so the thermal distribution computed for $U=0$ is a reasonable approximation. If two bodies with thermal conductivities $\kappa1$ and $\kappa2$ are in frictional contact on a disk of radius R and it is assumed that the temperature is continuous across the contact from one material to the other the maximum temperature of the contact can be estimated from Eq. (4). The total heat flux generated at the contact is

$$Q(t)=\frac{\mu N v(t)}{A} \tag{5}$$

where N is the normal force, $v(t)$ is the velocity of the contact and A is the contact area. Since gravity provides the driving force in our measurements, the acceleration of the block is constant with $a=g(\sin\theta-\mu\sqrt{2}\cos\theta)$, such that $v(t)=at$. A portion of this heat flux enters body 1 with $q1(t)=\kappa1Q(t)/(\kappa1+\kappa2)$, with the remainder $q2(t)=\kappa2Q(t)/(\kappa1+\kappa2)$ going into body 2. If the thermal conductivities of the two materials are the same, the heat flux is equally divided between the two bodies, but if the thermal conductivities differ substantially most of the heat flows into the body with the higher thermal conductivity. The maximum temperature rise at the interface is

$$\Delta T_{max}=\frac{RQ(t)}{(\kappa1+\kappa2)}=\frac{\mu N v(t)}{\pi R(\kappa1+\kappa2)} \tag{6}$$

The maximum temperature rise of the interface is predominately determined by the highest thermal conductivity between the two bodies in contact and is inversely proportional to the radius of the contact. Corrections to this formula for finite values of the Peclet number are given in [40].

Since the maximum flash temperature ΔT_{max} is inversely related to the thermal conductivity, it is important to understand the behavior of κ as a function of temperature in the cryogenic regime. Fig. 6 shows the thermal conductivities for sapphire and steel over the temperature range of this experiment [41,42]. The qualitative behavior of these curves is representative of crystalline insulators and metallic alloys. The kinetic gas model yields an expression for the thermal conductivity $\kappa=\frac{1}{3}Cv\ell$ where C is the heat capacity, v is the velocity of the thermal carrier (electrons or phonons), and ℓ is the mean free path. The velocity of the electrons and phonons are essentially independent of temperature. At $T=0$, the heat capacity and therefore also the thermal conductivity goes to zero. At low temperatures, the heat capacity of a crystalline insulator is $C\sim T^3$, while for a metal, $C\sim T$, so these power law dependencies govern the low temperature thermal conductivity as well. For a crystalline insulator, the thermal conductivity reaches a maximum and then decreases with increasing temperature because an increasing number of phonon-phonon collisions decreases the mean free path. For a metallic alloy, the mean free path is determined by impurities and is independent of temperature resulting in a thermal conductivity is approximately linear in T.

The above analysis shows that our apparatus is always in the low Peclet number limit, and that the local flash temperature rise is given approximately by Eq. (6). The temperature rise is determined primarily by the thermal conductivity, which varies by orders of magnitude as a function of temperature and from one material to another. Using the average heat flux during a sliding event in this experiment in Eq. (4), ΔT_{max} is 82 K for a steel/moly interface at 4 K while a sapphire/moly contact results in $\Delta T_{max}=$ 3.1 K. These upper bound calculations show that the flash temperature rise can greatly exceed the ambient temperature, particularly for materials such as steel with relatively low thermal conductivity. In an effort to estimate the flash temperature more accurately, finite element software (Comsol) was used to solve the heat diffusion equation for a realistic spherical contact geometry, accurate time dependence of the heat flux, and temperature dependent thermal parameters. Time evolved Comsol solutions of the temperature rise starting at the ambient temperature of 4 K are shown in Fig. 7(a) and (b) for the duration of a single slide event of 0.2 s duration at 50 ms intervals. These results show flash heating of 24.7 K for the steel interface and 2 K for the sapphire

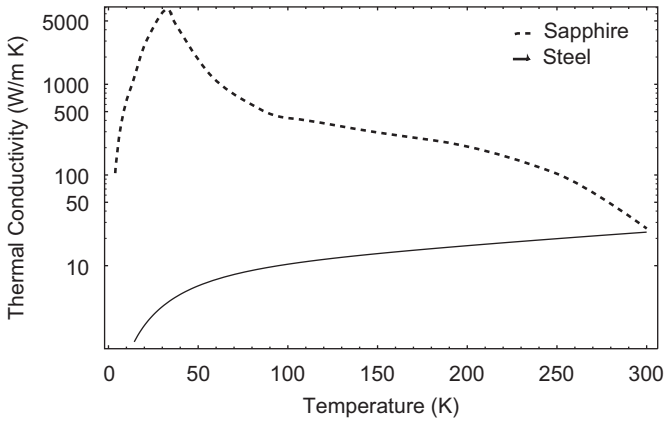

Fig. 6. The thermal conductivity of sapphire [42] increases with temperature below 35 K at which point the rate of phonon–phonon collisions reduces the mean free path resulting in decreasing thermal conductivity at higher temperatures. The very short electron mean free path in steel is unaffected by phonon collisions until temperature that exceed the experimental range of this experiment. The thermal conductivity of steel [41] from 4–300 K increases linearly in proportion to the heat capacity of the electron carriers. Flash heating increases at lower temperatures in alloy systems such as steel as a result of reduced thermal conductivity.

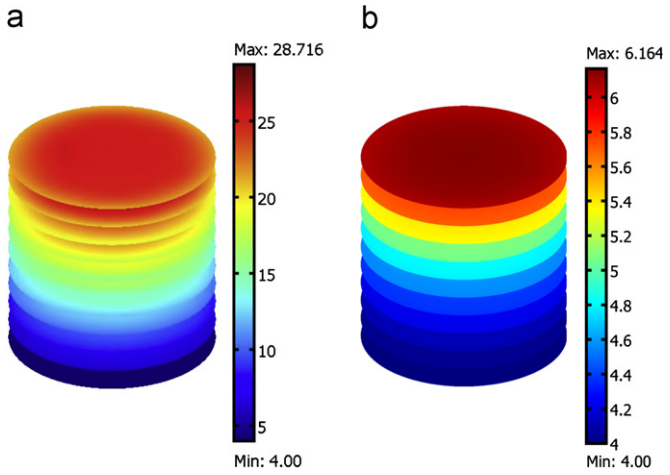

Fig. 7. Finite element (Comsol) solution for the time evolution of the temperature change in the circular contact area of radius 9 μm on a spherical bearing of radius 1.6 mm due to sliding friction that begins at $t=0$ with material properties of (a) being those of a steel bearing and (b) a sapphire bearing. The temperature is computed for 10 times which are 50 ms apart. The initial (ambient) temperature is 4 K (dark blue), but the upper end of the temperature scale (red) is different in (a) and (b). The calculation accounts for the differential thermal conductivity (in accordance with Eq. (6)) with total heat flux averaged over a linear time dependence of 3×10^6 and 7×10^6 W/m^2 for the steel and sapphire interfaces respectively. The resulting flash heating of the bearings places an upper bound on the change of temperature of the interface contact of 24.7 K for steel and 2.2 K for sapphire. (For interpretation of the references to color in this figure legend, the reader is referred to the web version of this article.)

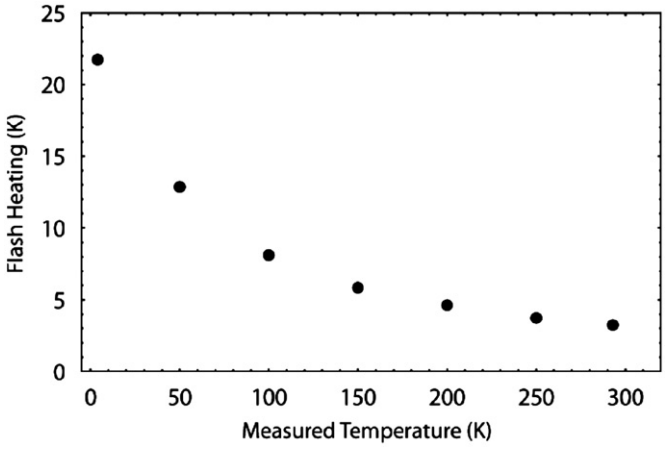

Fig. 8. The maximum temperature increase as a result of flash heating from finite element solutions is shown as a function of ambient temperature for a steel/moly sliding contact with geometries similar to those in this experiment. The model incorporates the temperature dependent thermal properties of steel and shows that flash temperature increases as the ambient temperature decreases. This complicates an analysis of temperature dependence of friction as the thermal behavior at the contact increasingly deviates from the measured ambient temperature as this temperature is decreased.

interface. Comsol solutions were obtained for the full temperature range of this experiment to better understand the larger effect at the steel/moly interface and are shown in Fig. 8. This analysis indicates that the temperature rise from flash heating in the steel/moly interface becomes relatively large as the ambient temperature approaches absolute zero, but for ambient temperatures above 100 K, flash heating raises the local temperature by less that 10 K.

The sliding block tribometer described above utilizes relatively low loads and low velocities, so the instantaneous heat flux at the contact is correspondingly low. The average heat flux into the track is extremely low because the time between slides is many minutes. Conventional pin-on-disc, reciprocating tribometers typically employ higher loads and, because of their steady motion, have orders of magnitude higher average heat flux into the substrate [1,43]. For some operating parameters the contact temperature can reach several hundred Kelvin above ambient [36–39] and the temperature rise becomes progressively larger at lower temperatures because of the reduced thermal conductivity in all but the most pure and highly crystalline materials. This analysis indicates that the selection of contact interface materials, load, velocity, and length of sliding time are all key parameters determining the increase in contact temperature resulting from friction. Furthermore, a detailed thermal analysis for each unique experimental setup is necessary to properly interpret and compare measurements.

3. Results

Fig. 2 shows the initial wear-in for the molybdenum disulfide + titanium coating. This preliminary experiment at room temperature, pressure and humidity shows that the friction coefficient is initially above 0.02 and quickly rises to 0.06 after roughly 100 runs, remaining constant thereafter. This is consistent with previous measurements of MoS_2 at room temperature in low humidity conditions [31] where the coating is reported to maintain this low friction state for thousands of cycles [26,25].

After evacuating the test chamber, several thermal cycles from 300 K to 4 K and back were performed. Fig. 9 shows the coefficient of kinetic friction as a function of the temperature of the tribometer for the steel/moly interface. The data demonstrate the repeatability and precision of the measurements in both directions of the thermal cycle. The coefficient of kinetic friction for steel has a roughly constant, average value of 0.04 between 300 K and 240. The coefficient of friction subsequently increases roughly linearly to a value of 0.125 at the measured track temperature of 4 K.

The sapphire/moly sliding contact showed a wider range of behavior between cycles. The initial cool down showed very high friction with a monotonic increase with decreasing temperature, while the subsequent warmup showed a sudden drop in the

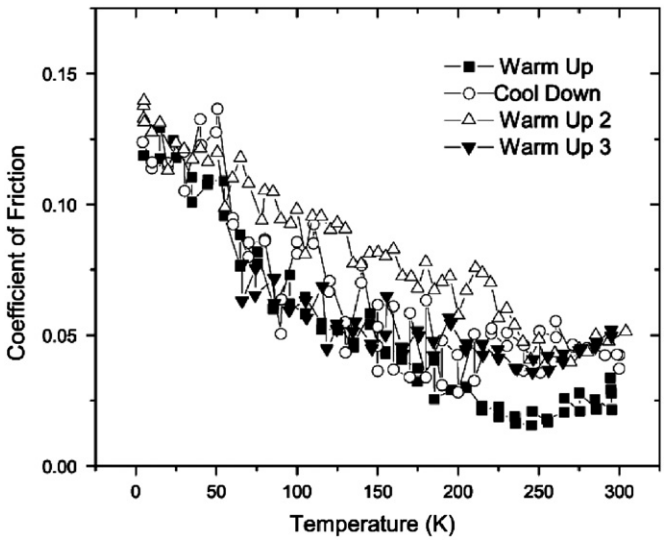

Fig. 9. The coefficient of kinetic friction for steel on MoS_2 + Ti as a function of the track (moly) temperature. The friction coefficient decreases slightly (if at all) from the value of $\mu=0.04$ with temperature from 300 K to 240 K, then increases roughly linearly to $\mu=0.125$ at 4 K. The trend in the data is repeatable for increasing or decreasing temperature and over multiple thermal cycles. The temperature of the contact may be up to 20 K higher than the track temperature.

coefficient of friction at ~125 K from a value of approximately 0.22 down to 0.1 at 125 K. Subsequent runs contributed to a generalized result of high friction at low temperature that monotonically reduces as the temperature is increased, similar in behavior to the steel/moly interface. The high temperature behavior was particularly variable which we hypothesize is a result of inconsistent transfer film bonding to the sapphire. The results are shown in Fig. 10.

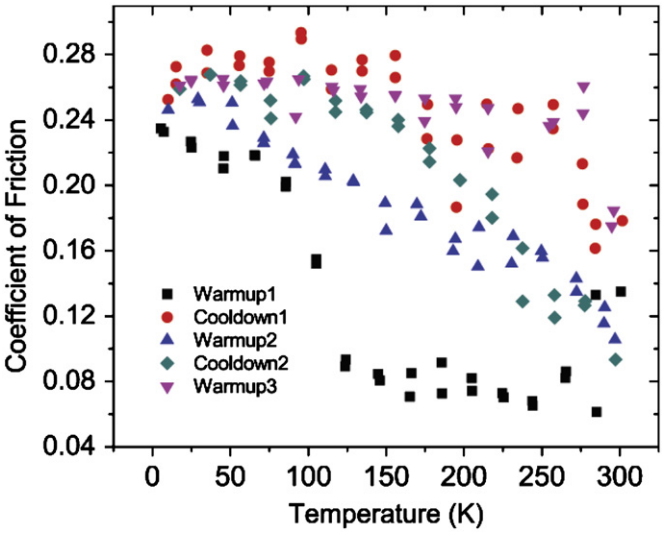

Fig. 10. The coefficient of kinetic friction for sapphire on MoS_2 + Ti as a function of the track (moly) temperature. The coefficient of kinetic friction decreases monotonically with increasing temperature from a low temperature value of $\mu = 0.25$ to a room temperature value in the range of 0.1–0.2. The basic behavior of low friction values at higher temperatures and high values at low temperatures is repeatable for increasing or decreasing temperature and over multiple thermal cycles. The temperature of the contact is expected to be within 2 K of the temperature of the track. The large variations in these measurements are presumably due to transfer film dynamics.

After all friction measurements were taken, the molybdenum disulfide + titanium plates were removed from the tribometer and observed under a Hyphenated Systems HS200 OP optical profiler in an attempt to determine the wear volume. Although a few isolated scratch marks were visible, no feature with a lateral scale on the order of the Hertzian contact size of 10 μm corresponding to a wear track was observed.

4. Discussion and conclusion

We have measured the kinetic friction of steel/MoS_2 + Ti and sapphire/MoS_2 + Ti interfaces in ultra-high vacuum from $T = 300$ K to 4 K. In both cases the friction increases monotonically with decreasing temperature, with the low temperature friction nominally three times greater than the room temperature value. Our values of the room temperature friction coefficient are in reasonable agreement with previous measurements in vacuum. Despite the large differences in the thermal and electrical properties of steel and sapphire, the tribological behavior as a function of temperature is similar. This is somewhat expected because lubrication in MoS_2 composites is due to the formation and dynamics of a transfer film [44]. The wear-in processes, however, seem to be quite different as a stable coefficient is reached for the case of steel but not sapphire. The specific mechanics involved in the formation of transfer films are not well understood but it is clear that more reactive transition metal surfaces form better films than less reactive surfaces [45]. We take our observations to indicate the transfer film on the sapphire bearings is weakly bound compared to that on the steel bearings and is periodically removed and reformed at the sliding contact. Our measurements appear to be in the near wear-less regime. Previous measurements of the wear rate for molybdenum disulfide + titanium coatings at room temperature yield a value less than 4×10^{-8} $(mm)^3/N\,m$ [26,46]. At this wear rate, the depth of the track after 1000 sliding events, which exceeds the number of events in this experiment is expected to be on the order of 0.01 nm, which is below a single molecular layer, and three orders of magnitude

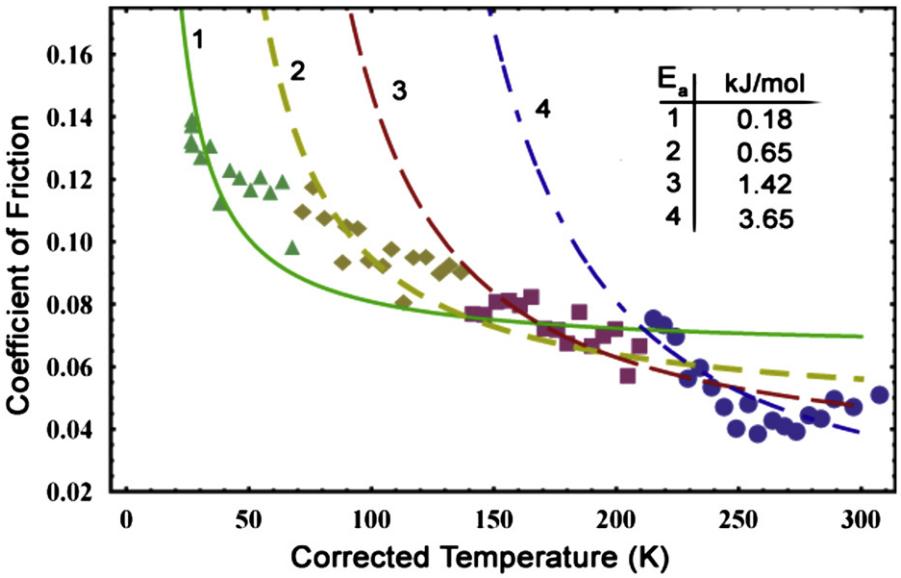

Fig. 11. Friction coefficient for a steel/MoS_2+Ti contact as a function of temperature that has been corrected for flash heating using the values from Fig. 8. The data are from Warmup 2 from Fig. 9; the data points have been divided into clusters, with the blue circles corresponding to $T > 210$ K, the red squares correspond to $210 < T < 130$ K, the yellow diamonds correspond to $60\text{ K} < T < 130$ K, and the green triangles correspond to $4\text{ K} < T < 60$ K. Curves are best fits to an Arrhenius functional form using various subsets starting with $T > 210$ K adding the subsequent sets at lower temperatures incrementally. The curves are labeled with their associated activation energies from each fit. The Arrhenius model is clearly unsuitable when all data are considered. (For interpretation of the references to color in this figure legend, the reader is referred to the web version of this article.)

smaller than the roughness of the MoS_2 film of 80 nm. The lack of an observable wear track in our experiment is consistent with previous measurements.

There are no previous measurements of the low temperature friction coefficient for MoS_2 + Ti in vacuum that we are aware of. Perhaps the closest related study is Hamilton et al. [9] who measured the friction coefficient of steel/MoS_2 in a dry nitrogen environment in the temperature range 200 K < T < 430 K using a reciprocating pin-on-disk tribometer. Our results are in good agreement at high temperature, but Hamilton et al. see an abrupt rise in friction below T=240 K by about a factor of three. Our data also show an increase of μ by approximately a factor of three from room temperature to 4 K, but the behavior is smooth and varies approximately linearly with the temperature. The measurements differ both because of the ambient gas pressure and also because of the potential contact flash heating as discussed previously. Hamilton et al. and similar work by McCook et al. on PTFE [1] used an Arrhenius equation $\mu = \mu_0 e^{Ea/(RT)}$ to extract an activation energy, Ea, to fit their results. A similar analysis performed with our steel/moly data is shown in Fig. 11. An Arrhenius function necessarily diverges at low temperatures unlike the behavior observed in this experiment; however, best fit parameters can nevertheless be found for data at high temperatures. The fit parameters are quite sensitive to the subset of the data that are used to construct the fit. For example, using only the data with T > 210 K yields a reasonable fit with Ea=3.65 kJ/mol, which is similar to the values obtained by Hamilton et al. of several kJ per mole. Extending the range to T > 130 K yields a less satisfying fit with a significantly lower value of Ea=1.42 kJ/mol. Including an even wider range of temperatures yields much smaller activation energies and a lower quality fit. The activation energy is largely determined by the low temperature cutoff of the data set, but it appears to be a very poor predictor of the data at temperatures even slightly lower than the cutoff. We conclude that the Arrhenius analysis is not a useful model to describe the temperature dependence of friction.

Our results demonstrate that MoS_2 + Ti films can survive thermal cycling from room temperature to cryogenic temperatures in UHV and will retain their tribological utility with very low wear. Molybdenum disulfide based coatings provide a robust and practical solution to the problem of lubrication in vacuum at cryogenic temperatures. The friction coefficient of steel/ MoS_2 + Ti is lower than the friction coefficient of steel/PTFE [22] for all temperatures below room temperature. Although conventional pin-on-disk tribometers operated at low temperatures can simulate realistic conditions of engineering importance, the continuous motion in these tribometers leads to steady state flash temperature maximums that can greatly exceed the ambient temperature. For this reason, conventional continuous motion tribometers are not well suited for fundamental studies of friction when precise knowledge of the interfacial temperature is important. Furthermore, a thorough analysis of flash heating must accompany data to accurately link the temperature dependence of friction to theoretical models.

Acknowledgments

This work was supported by *EXTREME FRICTION* AFOSR MURI # FA9550-04-1-0381 and NSF DMR-0907495.

References

[1] McCook NL, Burris DL, Dickrell PL, Sawyer WG. Cryogenic friction behavior of PTFE based solid lubricant composites. Tribol Lett 2005;2(2):109–13.
[2] Leger LJ, Dufrane K. Space station lubrication considerations. In: The 21st aerospace mechanisms symposium; 1987. p. 285–294.
[3] Zhang X, Vitchev RG, Lauwerens W, He J, Celis J-P. Transfer of molybdenum sulphide coating material onto corundum balls in fretting wear tests. Thin Solid Films 2004;446:78–84.
[4] Winer WO. Molybdenum disulfide as a lubricant: A review of the fundamental knowledge. Wear 1967;10(6):422–52.
[5] Roberts EW. Thin solid lubricant films in space. Tribol Int 1990;23:95–104.
[6] Michael PC, Rabinowicz E, Iwasa Y. Thermal activation in boundary lubricated friction. Wear 1995;193(2):218–25.
[7] Theiler G, Hubner W, Gradt T, Klein P, Friedrich K. Friction and wear of PTFE composites at cryogenic temperatures. Tribol Int 2002;35:449–58.
[8] Hubner W, Gradt T, Schneider T, Borner H. Tribological behaviour of materials at cryogenic temperatures. Wear 1998;216(2):150–9.
[9] Hamilton MA, Alvarez LA, Mauntler NA, Argibay N, Colbert R, Burris DL, et al. A possible link between macroscopic wear and temperature dependent friction behaviors of MoS2 coatings. Tribol Lett 2008;32:91.
[10] Yukhno TP. Low temperature investigations on frictional behavior and wear resistance of solid lubricant coatings. Tribol Int 2001;34:293–8.
[11] Popov VL. Superslipperiness at low temperatures: Quantum mechanical aspects of solid state friction. Phys Rev Lett 1999;83:1632–5.
[12] Krylov SY, Jinesh KB, Valk H, Diewiebel M, Frenken JWM. Thermally induced suppression of friction at the atomic scale. Phys Rev E 2005;71:65101.
[13] Schirmeisen A, Jansen L, Holscher H, Fuchs H. Temperature dependence of point contact friction. Appl Phys Lett 2006;88:123108.
[14] Zhao X, Hamilton M, Sawyer WG, Perry SS. Thermally activated friction. Tribol Lett 2007;27:113–7.
[15] Barel I, Urbakh M. Multibond dynamics of nanoscale friction: the role of temperature. Phys Rev Lett 2010;104:066104.
[16] Dunckle CG, Altfeder IB, Voevodin AA, Jones J, Krim J, Taborek P. Temperature dependence of single-asperity friction for a diamond on diamondlike carbon interface. J Appl Phys 2010;107:114903.
[17] Brukman MJ, Gao G, Nemanich RJ, Harrison JA. Temperature dependence of single-asperity diamond—diamond friction elucidated using AFM and MD simulations. J Phys Chem C 2008;112:9358–69.
[18] Bruschi L, Pierno M, Fois G, Ancilotto F, Mistura G. Friction reduction of ne monolayers on preplated metal surfaces. Phys Rev B 2010;81:11.
[19] Renner R, Rutledge J, Taborek P. Quartz microbalance studies of superconductivity-dependent sliding friction. Phys Rev Lett 1999;83:6.
[20] Harrison JA, White CT, Colton RJ, Brenner DW. Molecular-dynamics simulations of atomic-scale friction of diamond surfaces. Phys Rev B 1992;46(15):9700–8.
[21] Kapila V, Deymier PA, Raghavan S. Molecular dynamics simulations of friction between alkylsilane monolayers. Model Simul Mater Sci Eng 2006;14:283–97.
[22] Burton JC, Taborek P, Rutledge JE. Temperature dependence of friction under cryogenic conditions in vacuum. Tribol Lett 2006;23(2):131–7.
[23] Aggleton M, Burton JC, Taborek P. Cryogenic vacuum tribology of diamond and diamond-like carbon films. J Appl Phys 2009;106:013504.
[24] Barton GC, Pepper SV. Transfer of molybdenum disulphide to various materials. NASA TP 1997:1019.
[25] Teer D. New solid lubricant coatings. Wear 2001;251:1068.
[26] Fox VC, Renevier N, Teer DG, Hampshire J, Rigato V. The structure of tribologically improved MoS_2-metal composite coatings and their industrial applications. Surface Coat Technol 1999;116–119:492–7.
[27] Singer IL, Pollack HM. Fundamentals of friction: macroscopic and microscopic processes. The Netherlands: Kluwer Academic Publishers; 1992.
[28] Rutledge JE, Taborek P. Prewetting phase-diagram of He-4 on cesium. Phys Rev Lett 1992;69:937.
[29] Phillips JA, Ross D, Taborek P, Rutledge JE. Superfluid onset and prewetting of He-4 on rubidium. Phys Rev B 1998;58:3361.
[30] Haltner AJ, Oliver CS. Effect of water vapor on the friction of molybdenum disulfide. I&EC Fundam 1966;5(3):348–55.
[31] Lancaster J. A review of the influence of environmental humidity and water of friction, lubrication and wear. Tribol Int 1990;23:371.
[32] Beniya A, Yamamoto S, Mukai K, Yamashita Y, Yoshinobu J. The first layer of water on Rh(111): Microscopic structure and desorption kinetics. J Chem Phys 2006; 125, article 054717.
[33] Dounce SM, Jen SH, Yang M, Dai HL. The wetting–dewetting transition of monolayer water on a hydrophobic metal surface observed by surface-state resonant second-harmonic generation. J Chem Phys 2005; 122, article 204703.
[34] Chakarov DV, Österlund L, Kasemo B. Water adsorption on graphite (0001). Vacuum 1995;46(8–10):1109–12.
[35] Carslaw HS, Jaeger JC. Conduction of heat in solids. Oxford: Clarendon Press; 1978.
[36] Bowden FP, Tabor D. The friction and lubrication of solids. Oxford: Clarendon Press; 1950.
[37] Jaeger JC. Moving sources of heat and the temperature at sliding contacts. Proc R Soc New South Wales 1943;76:203–24.
[38] Archard J. The temperature of rubbing surfaces. Wear 1959;2:438–55.
[39] Wang Y, Rodkiewicz C. Temperature maps for pin-on-disk configuration in dry sliding. Tribol Int 1994;27(4):259–66.
[40] Tian XF, Kennedy FE. Maximum and average flash temperatures in sliding contacts. ASME J Tribol 1994;116:167–74.
[41] Mann D. LNG materials and fluids. Nat Bur Stand 1977.

[42] Pobell F. Matter and methods at low temperatures. Berlin, Heidelberg, New York: Springer; 2007.
[43] Gradt T, Börner H, Schneider T. Low temperature tribometers and the behaviour of ADLC coatings in cryogenic environment. Tribol Int 2001;34:225–30.
[44] Holinski R, Gansheimer J. A study of the lubricating mechanism of molybdenum disulfide. Wear 1972;19(3).
[45] Singer IL. In situ analysis of the tribiochemical films formed by SiC sliding against Mo in partial pressures of SO2, O2, and H2S gases. J Vac Sci Technol A 1996;14(1).
[46] Rigato V, Maggioni G, Patelli A, Boscarino D, Renevier NM. Surf Coat Technol 2000;206.